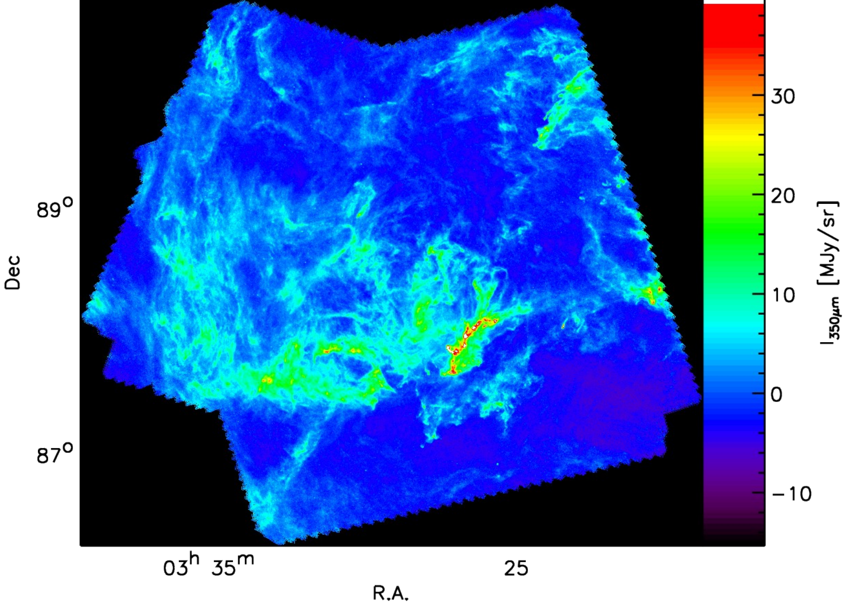

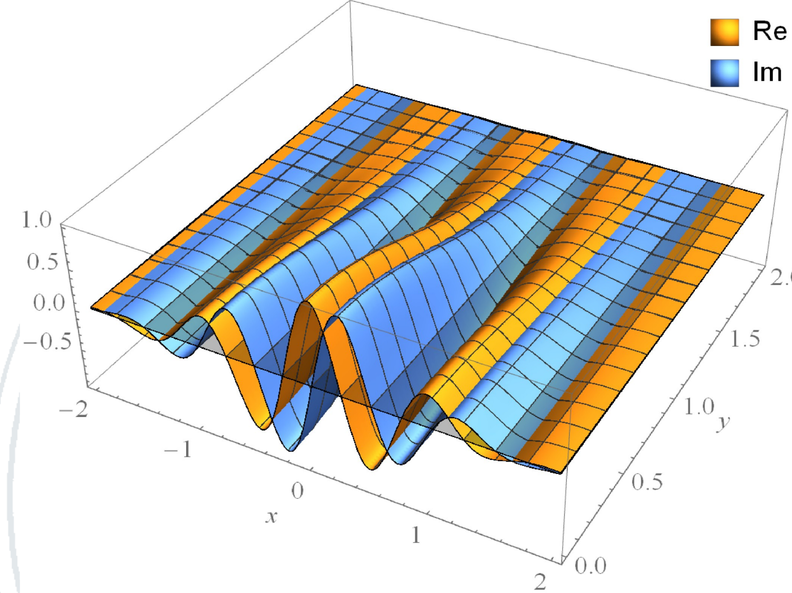

Measuring filaments through anisotropic wavelets

Volker Ossenkopf-Okada, Rodion Stepanov

Submitted to A&A

KOSMA
(**K**ölner **O**bservatorium für **S**ub**M**m **A**stronomie),
I. Physikalisches Institut, Universität zu Köln

Overview

- Motivation
  - Filament finders
- New tool
  - Δ-variance inheritance
  - Anisotropic wavelets
  - Tests
- Applications
  - MHD turbulence
  - Observations
  - Gravitational stability

Observations

- Filaments everywhere

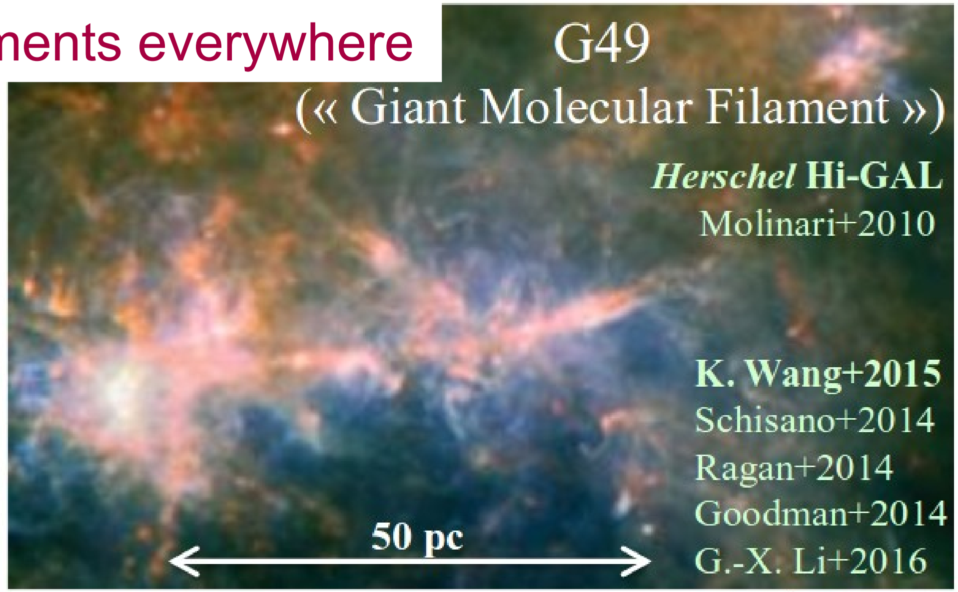

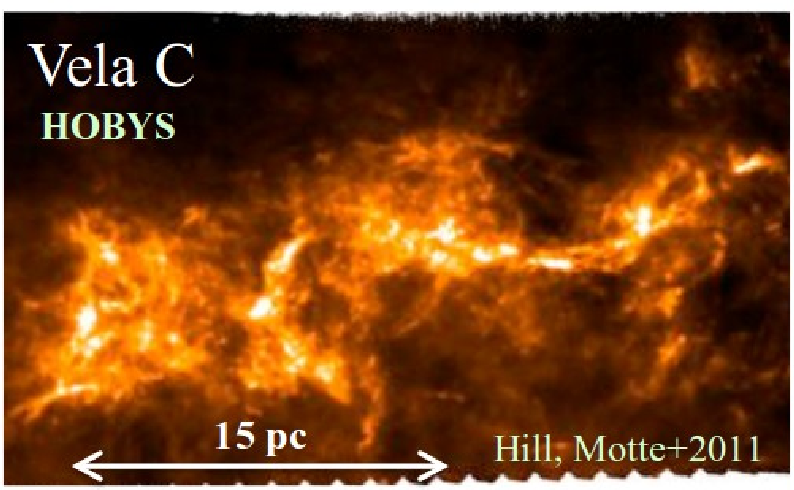

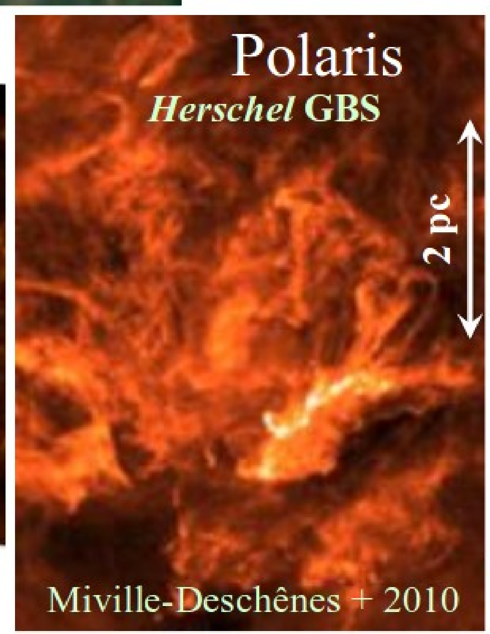

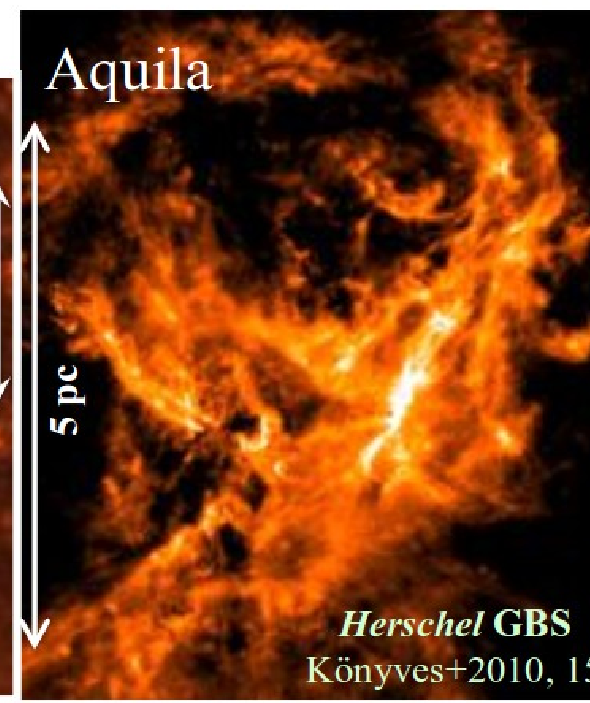

Ph. André - ISM2017 – Cologne– 13 Feb 2017

Formation

- 3 different processes discussed

Gravity-dominated cloud formation	Turbulent fragmentation	Magnetic-field guided sheet formation
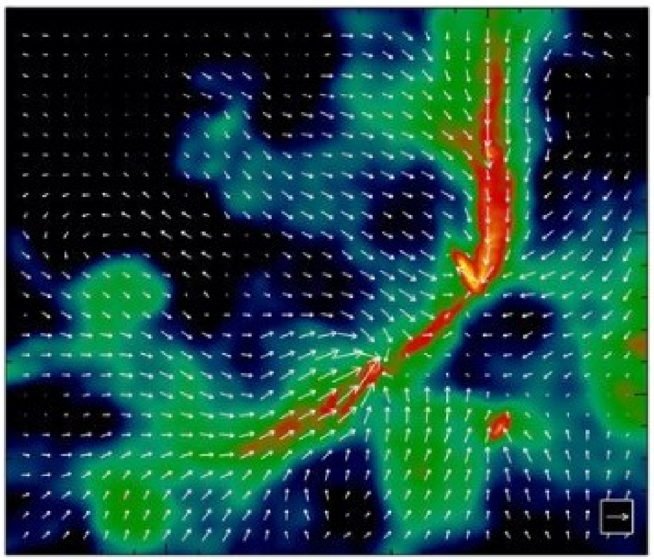	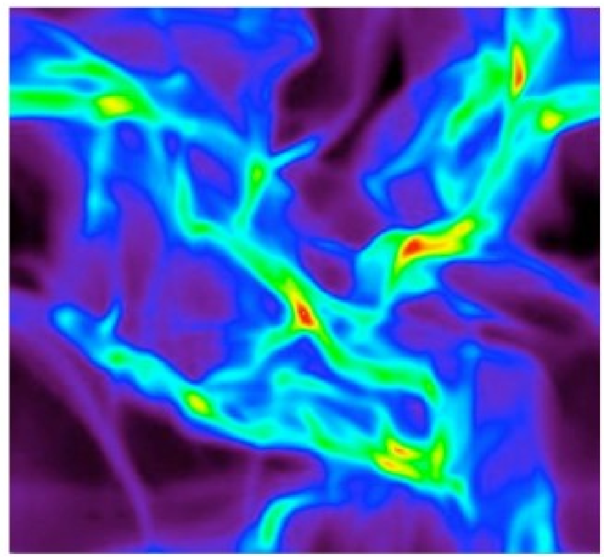	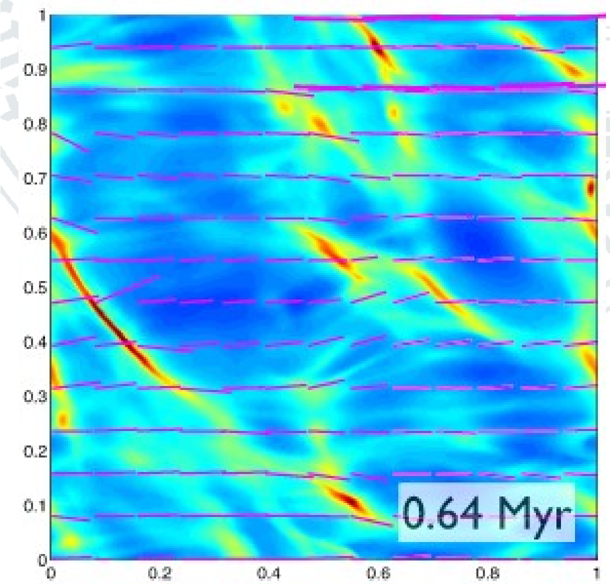
e.g. Gomez & Vazquez-Semadeni (2014)	e.g. Padoan et al. (2001), Pudritz & Kevlahan (2013)	e.g. Chen & Ostriker (2014), Inutsuka et al. (2015)

- Filaments produced in many processes
- Distinguishable by ratio of sheets to filaments and velocity structure in filaments

Filaments

How to quantify filaments

- Traditional approach
  - Look for peaks in curvature space and connect them → DisPerSe, getFilaments

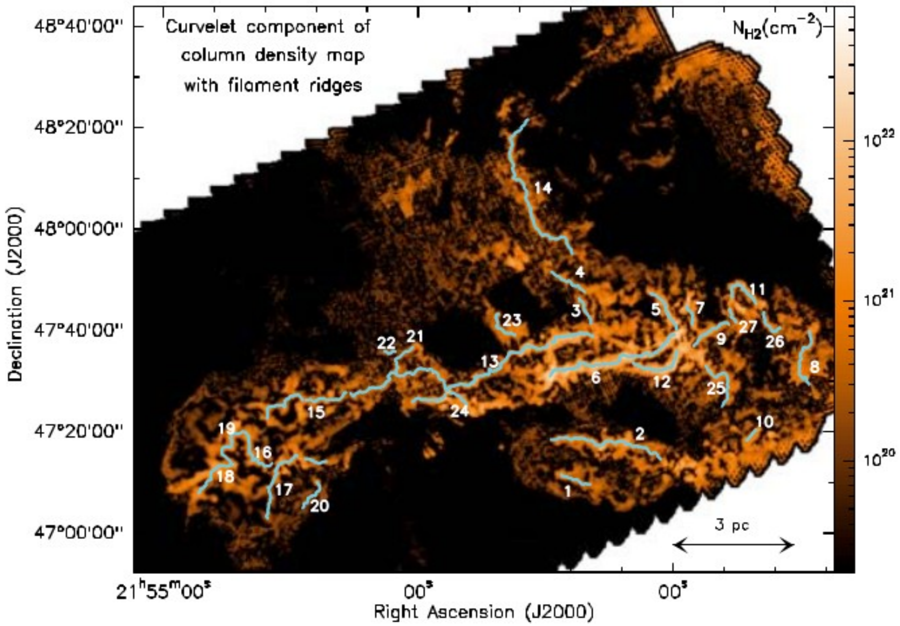

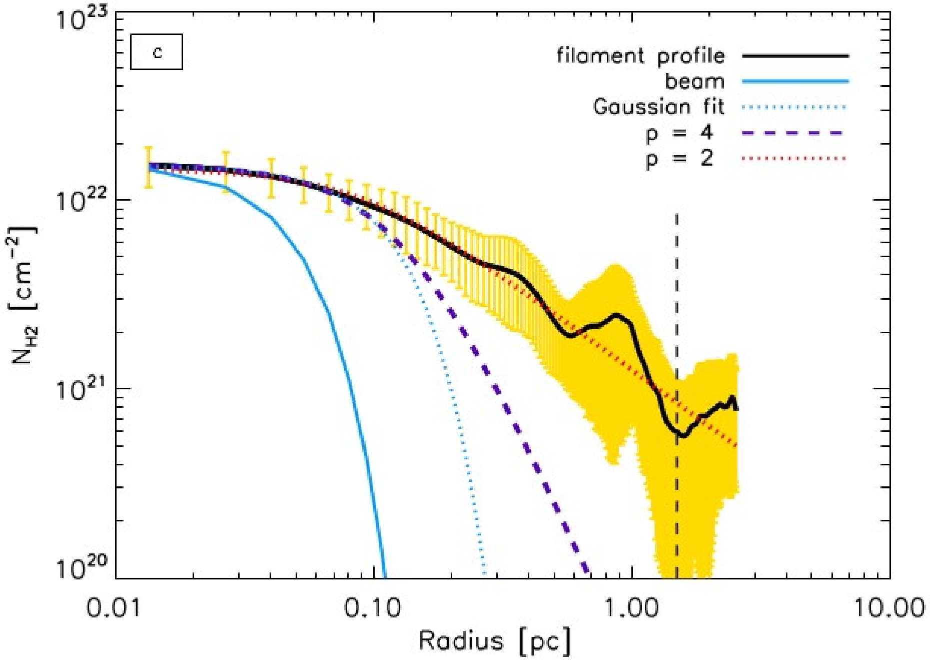

Arzoumanian et al. (2011)

  - Retrieves typical filament width (0.1pc) determined by scale/resolution used in the method (Panopoulou 2016), not by the underlying structure
  - Unbiased method required!

Use inheritance from Δ-variance

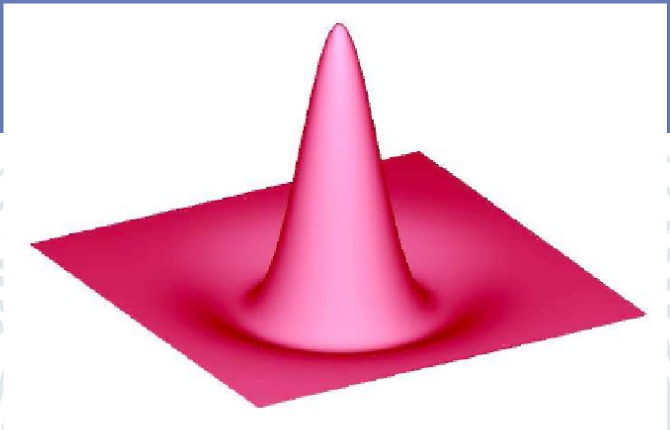

Measure spatial scaling:

Filter map by radially symmetric wavelet $\psi_l(r)$

- characteristic length scale *l*
- Measure variance in convolved image as function of the filter size *l*
- Gives relative amount of structure as a function of structure size
- Power-law power spectrum $P(k) \propto k^{-\beta}$ gives power-law Δ-variance $\sigma_\Delta^2(l) \propto l^\alpha$ with $\alpha = \beta - 2$

- **Advantages compared to power spectrum**
  - Δ-variance can measure spatial scaling of irregular maps, maps with variable noise.
  - In the application to observed maps the Δ-variance is much more robust.

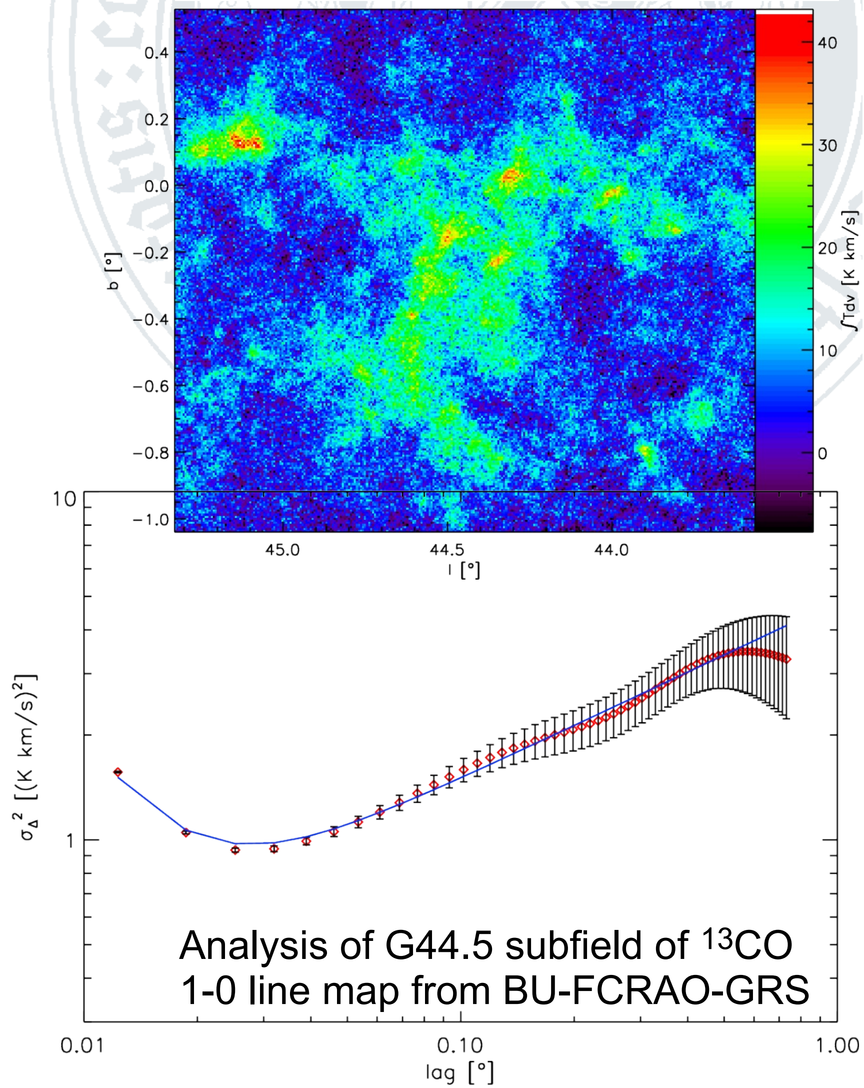

Analysis of G44.5 subfield of ^{13}CO 1-0 line map from BU-FCRAO-GRS

Equivalent approach for filaments

Anisotropic wavelet

- Convolution of the map $f(\mathbf{x})$: $W(s,\varphi,\mathbf{x}) = \frac{1}{s^{3/2}} \int_{-\infty}^{+\infty} \int_{-\infty}^{+\infty} f(\mathbf{x}) \psi_\varphi \left(\frac{\mathbf{x}' - \mathbf{x}}{s} \right) d\mathbf{x}'$

  with an anisotropic filter:

$$\psi_\varphi(\mathbf{x}) = \psi(x\cos\varphi - y\sin\varphi, x\sin\varphi + y\cos\varphi)$$

$$\psi(x,y) = \left[\exp(2\pi\imath x) - \exp(-\pi^2 b^2)\right] \exp\left(\frac{-x^2 - y^2}{b^2} \right)$$

- Compute maps of isotropic and anisotropic wavelet coefficients as a function of the filter size s:

$$m^i(s,\mathbf{x}) = (2\pi)^{-1} \int_{-\pi}^{+\pi} |W(s,\varphi,\mathbf{x})|^2 d\varphi,$$

$$m^a(s,\mathbf{x}) = (2\pi)^{-1} \int_{-\pi}^{+\pi} |W(s,\varphi,\mathbf{x})|^2 e^{2\imath\varphi} d\varphi$$

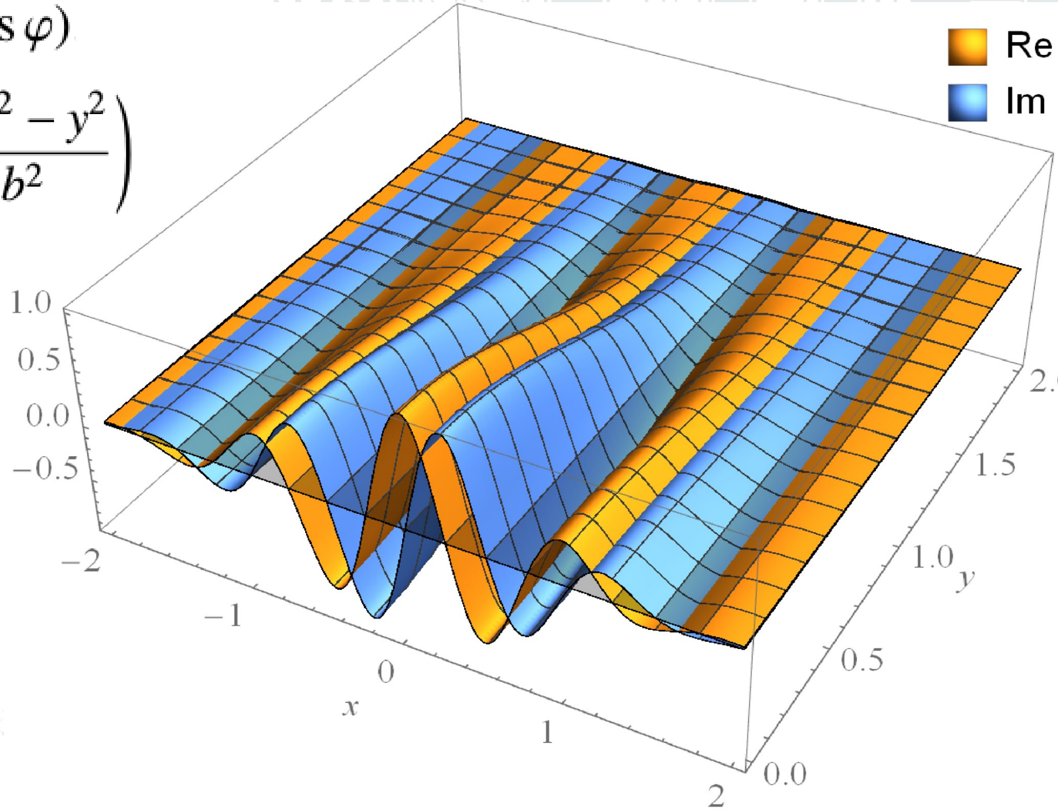

Wavelet spectra from spatial averages

- Isotropic and anisotropic wavelet spectra as function of the filter size *s*:

$$M^i(s) = \left\langle m^i(s,\mathbf{x})\right\rangle_{\mathbf{x}},$$
$$M^a(s) = \langle |m^a(s,\mathbf{x})|\rangle_{\mathbf{x}}$$

- Local and global degree of anisotropy:

$$d^w_{loc}(s) = M^a(s)/M^i(s)$$
$$d^w_{glob}(s) = \frac{|\langle m^a(s,\mathbf{x})\rangle_{\mathbf{x}}|}{M^i(s)}$$

- Orientation of the filaments

$$\varphi^w(s) = \frac{1}{2}\arg\left(\langle m^a(s,\mathbf{x})\rangle_{\mathbf{x}}\right)$$

- Provides
  - spatial and angular distribution of the wavelet coefficients
  - local and global degree of anisotropy as a function of the size scale

Artificial data sets

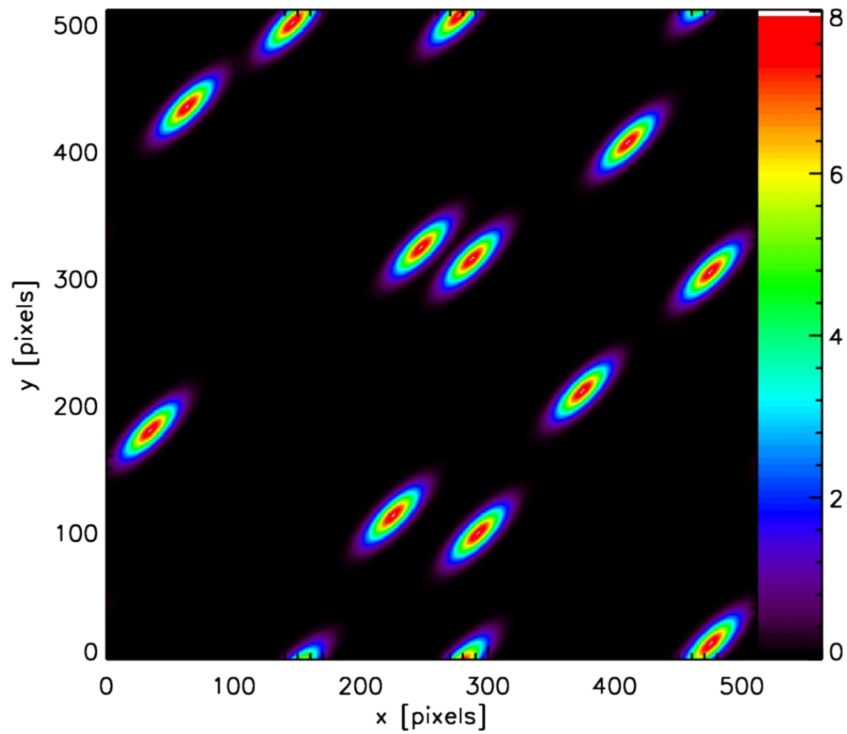

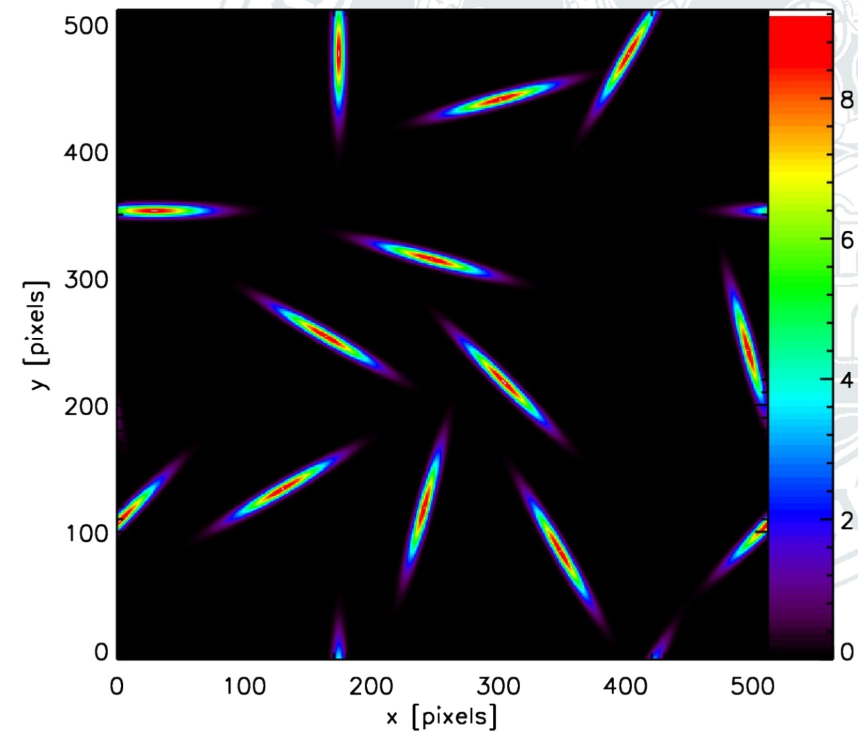

Example test data: ellipses with axes ratios 3:1 and 9:1, aligned or uniformly distributed

- Compute maps of isotropic and anisotropic coefficients with amplitude, angle and spatial distribution as a function of the wavelet scale
  - 4D result

Tests

Wavelet spectra

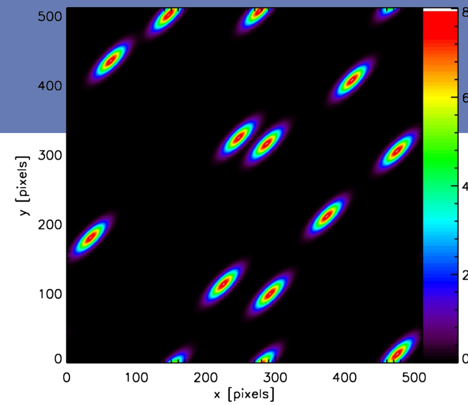

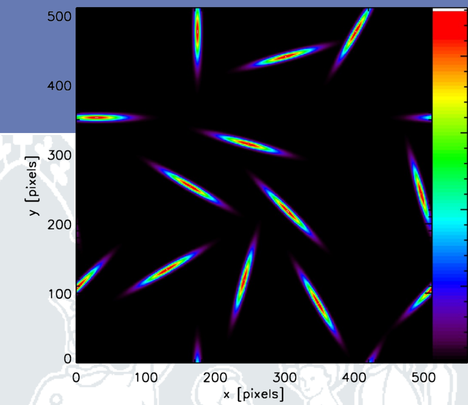

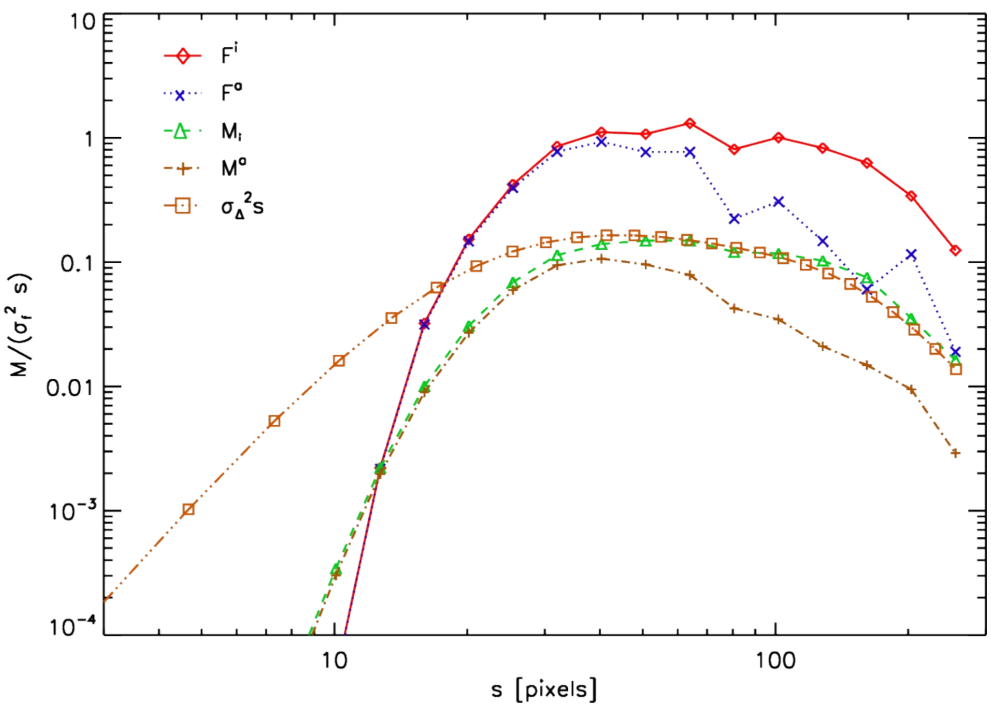

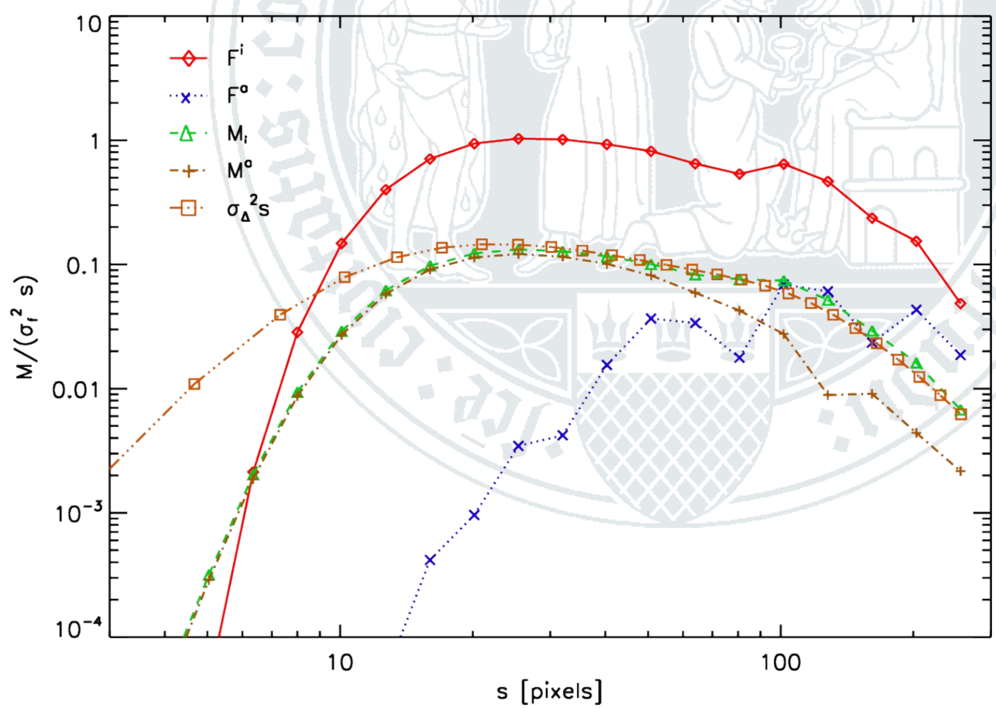

Wavelet spectra (isotropic- M^i, anisotropic -M^a) compared to Fourier spectra and Δ-variance

- Wavelet spectra have a better scale sensitivity than Δ-variance
- Anisotropic wavelets feel local anisotropy in contrast to power spectrum

Tests

Angular spectra

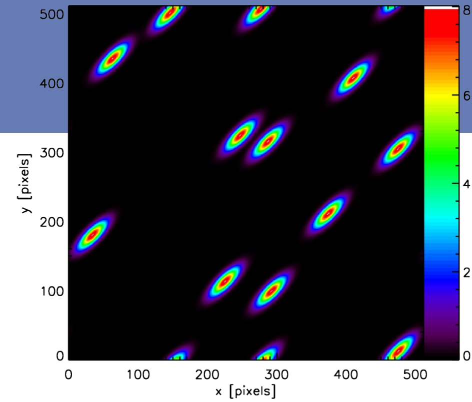

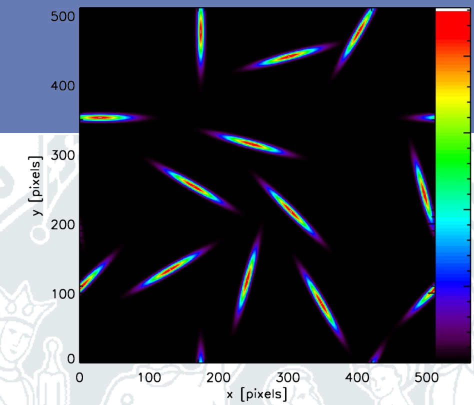

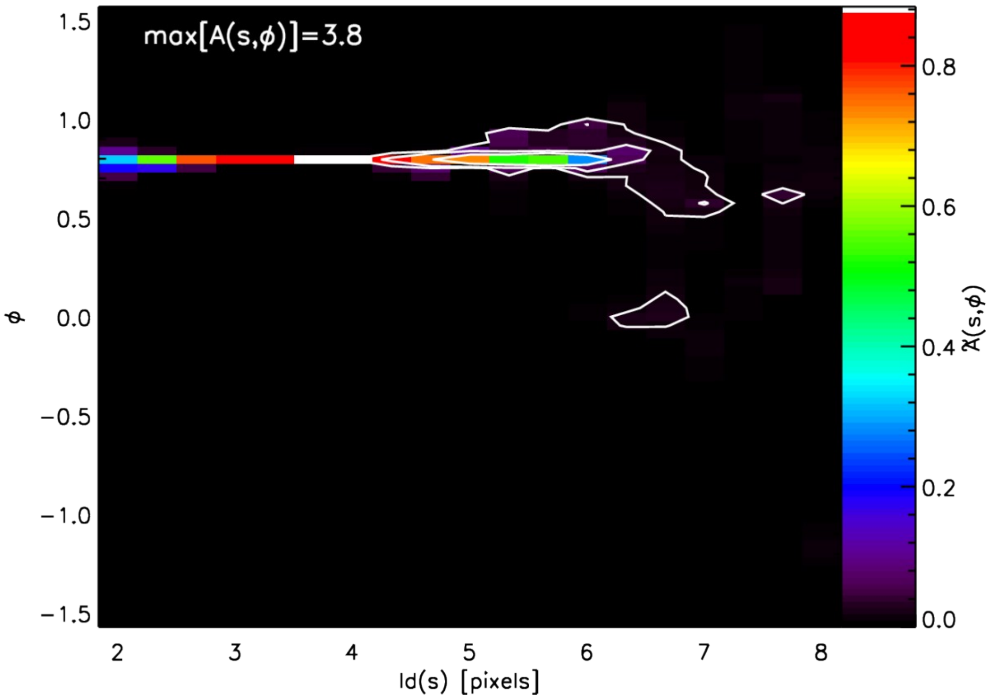

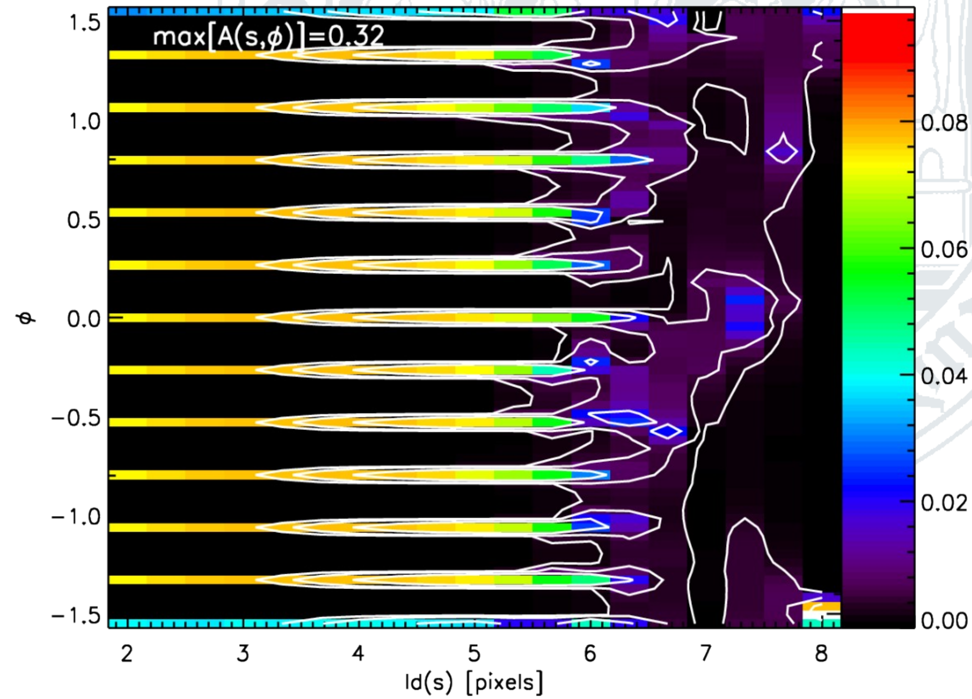

Angular spectra, colours are normalized to the isotropic coefficients M^i

- Sensitive measurement of angular distribution
  - π-ambiguity due to symmetry of the problem

Degrees of anisotropy

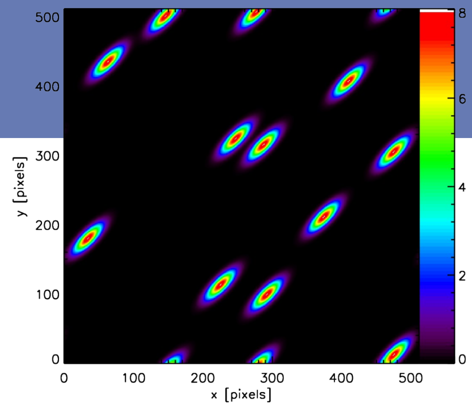

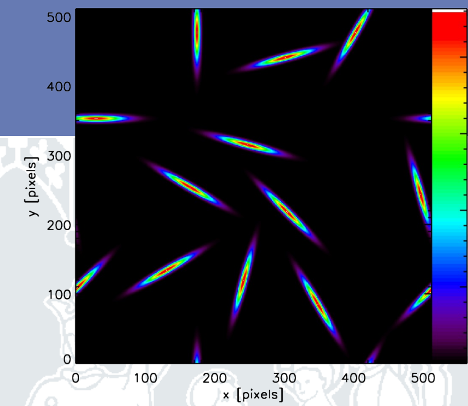

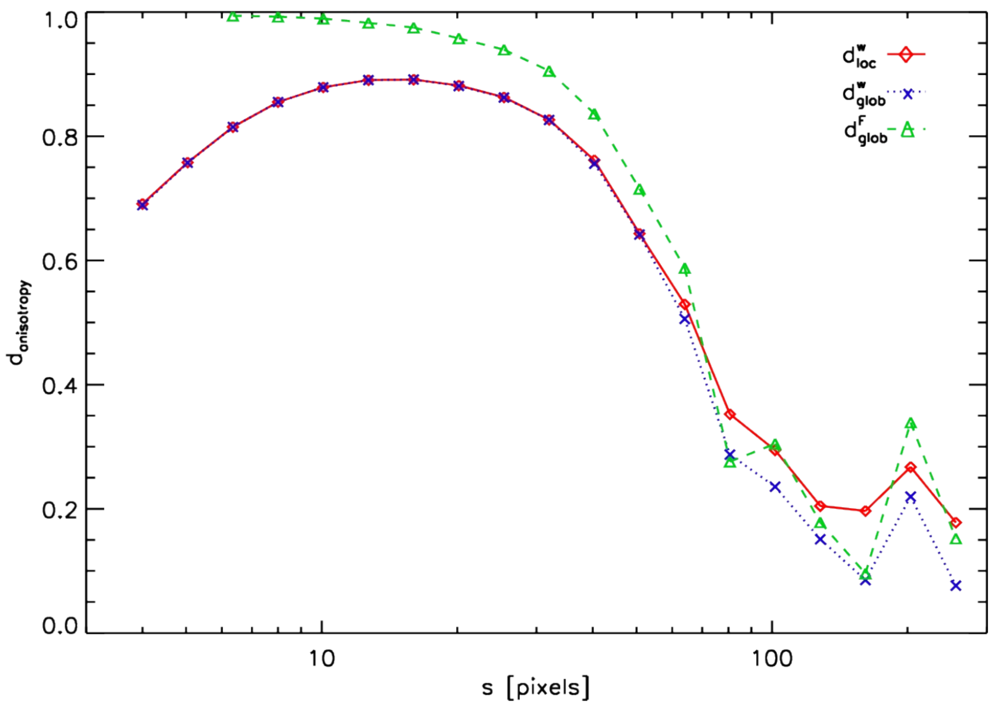

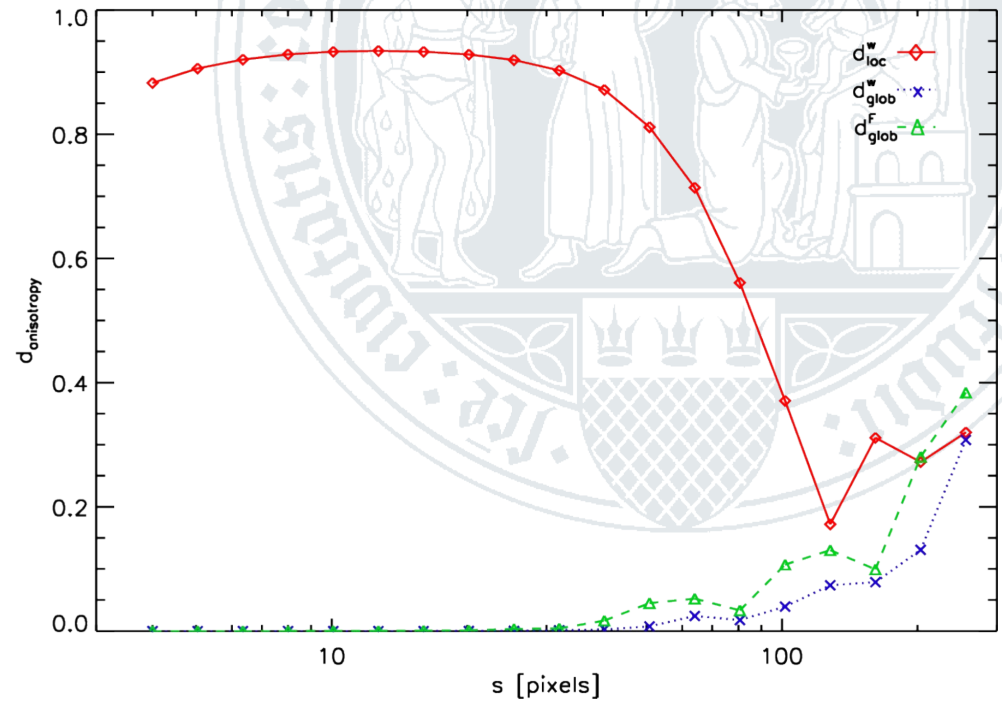

Local (red) and global (blue) degree of anisotropy from wavelet analysis and global degree from Fourier transform (green)

- Wavelet analysis shows anisotropy over limited range of scales
- Clear distinction between global and local anisotropy

Magnetohydrodynamic models

- Gas motion couples to magnetic field
- Different modes of wave propagations
- Large-scale asymmetries
- Filaments everywhere

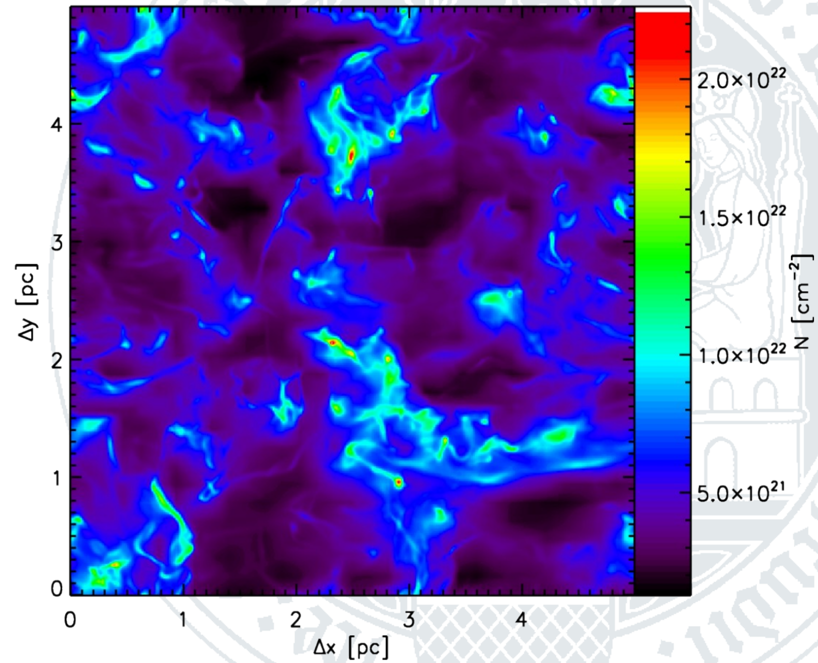

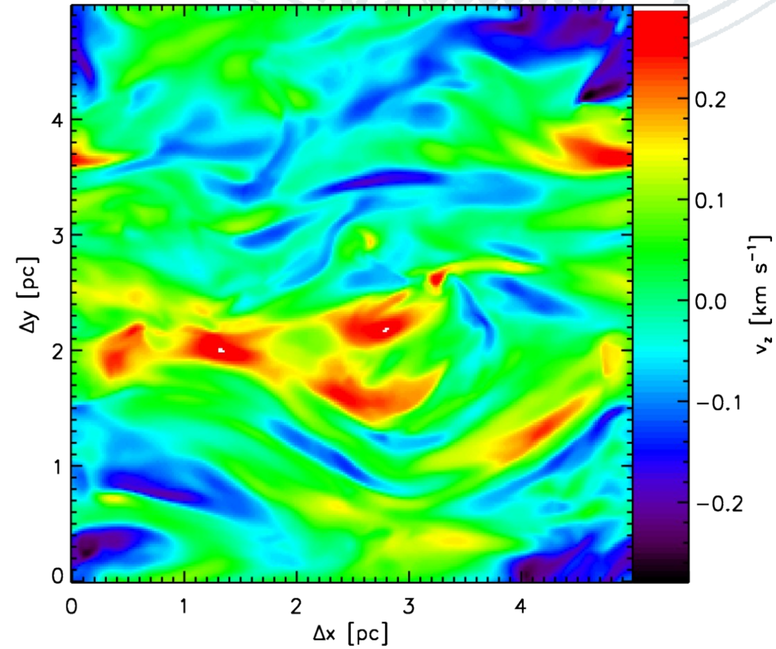

Column density structure (top) and velocity slice (bottom) in a supersonic, subalfvenic turbulence simulation (Burkhart et al. 2013)

Application to MHD simulations

Analysis of observable maps

Simulated CO 2-1 intensity maps from the MHD simulation:

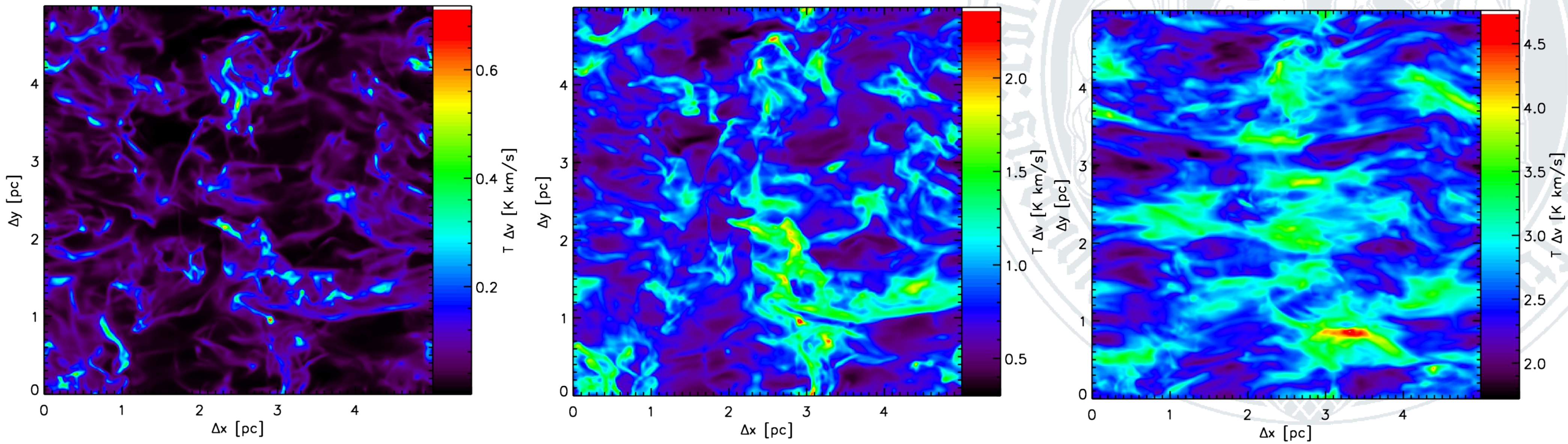

Integrated line intensity assuming different optical depth resulting from different molecular abundances:
$C^{18}O$: X=5 10^{-8}, ^{13}CO: X=1.5 10^{-6}, ^{12}CO: X=4.5 10^{-5}.

- All maps filamentary
- High optical depths emphasize the global anisotropy imprinted mainly on the velocity field (following the global magnetic field)

Application to MHD simulations

Degree of anisotropy as a function of size scale:

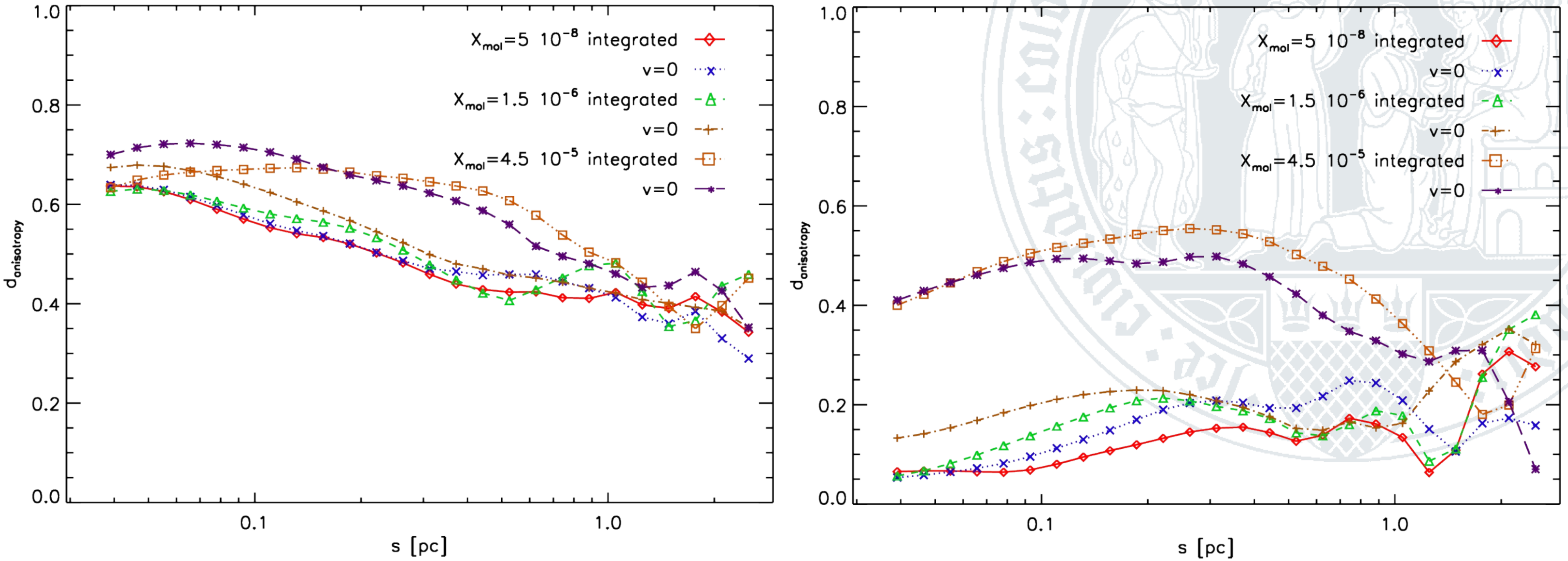

Spectra of the local (left) and global degree of anisotropy (right) for the three maps.

- High degree of local anisotropy from small filaments. For large optical depths global anisotropy becomes significant and filaments are wider. Filaments at low optical depth unaligned.
- Imprint of the magnetic field on the structure at all size scales. Small-scale filaments preferentially entangled with the field lines.

Observed column density maps from Herschel observations

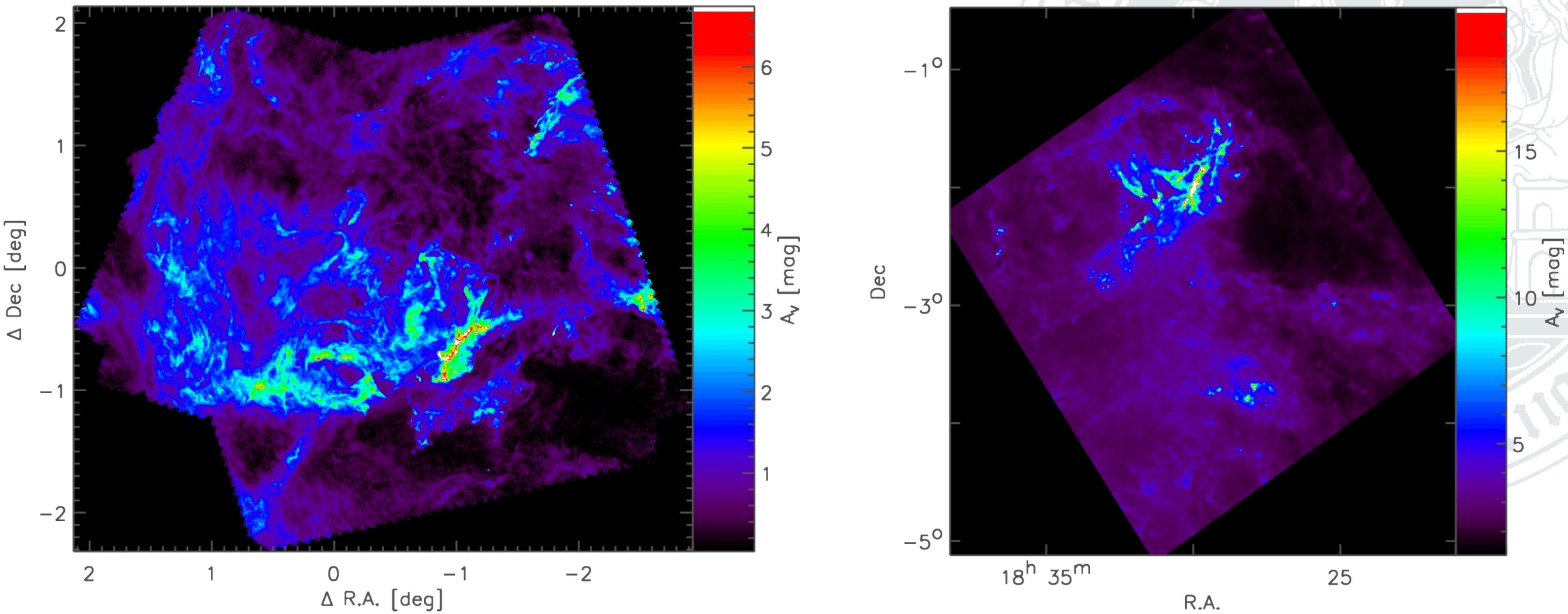

Filamentary dust maps of the Polaris (left) and Aquila (right) regions previously analysed by André et al. (2010), Schneider et al. (2013).

- In spite of the different nature of the clouds André et al. (2010) find a common filament width of 0.1pc for both clouds.

Polaris and Aquila

Wavelet spectra and degrees of anisotropy for both regions:

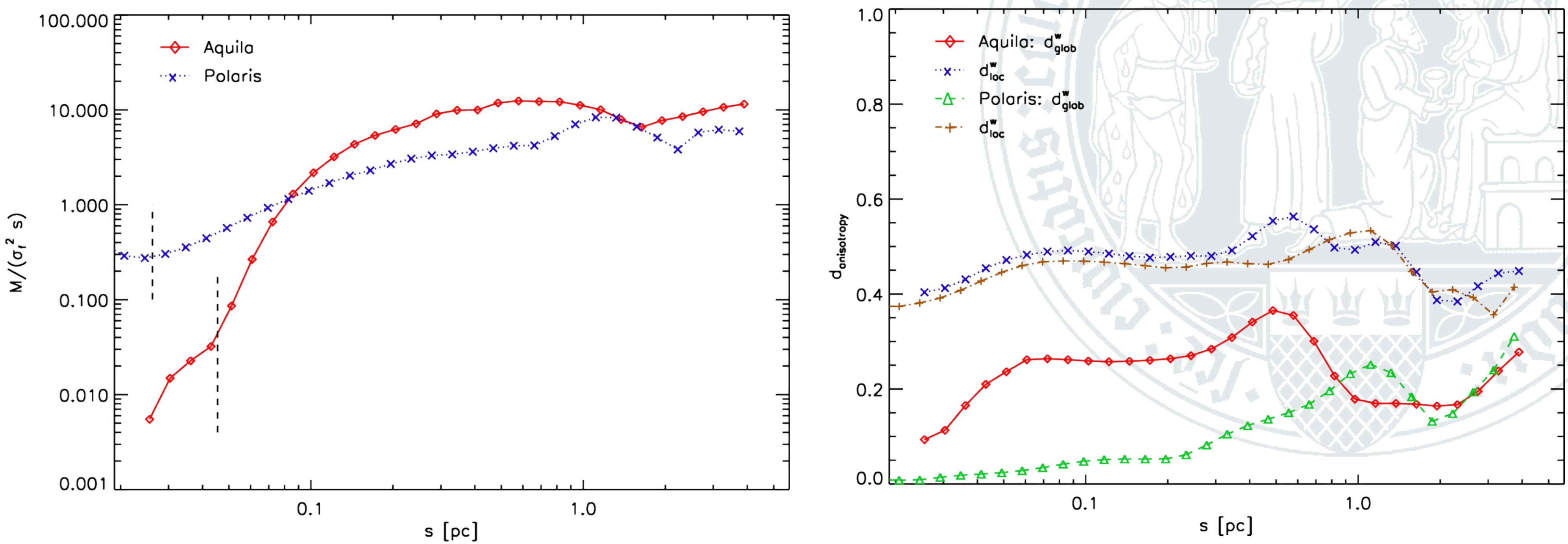

Isotropic and anisotropic wavelet coefficients (left) and local and global degrees of anisotropy (right) for the two maps. Dashed lines indicate the beam sizes.

- Polaris shows no characteristic size scale and no global anisotropy, but a high filamentariness measured by the local anisotropy at all scales.
- Aquila has an enhanced scales of anisotropy at 0.6-0.8 pc corresponding to a filament width of 0.3pc. The filaments are aligned producing global anisotropy.

Polaris and Aquila

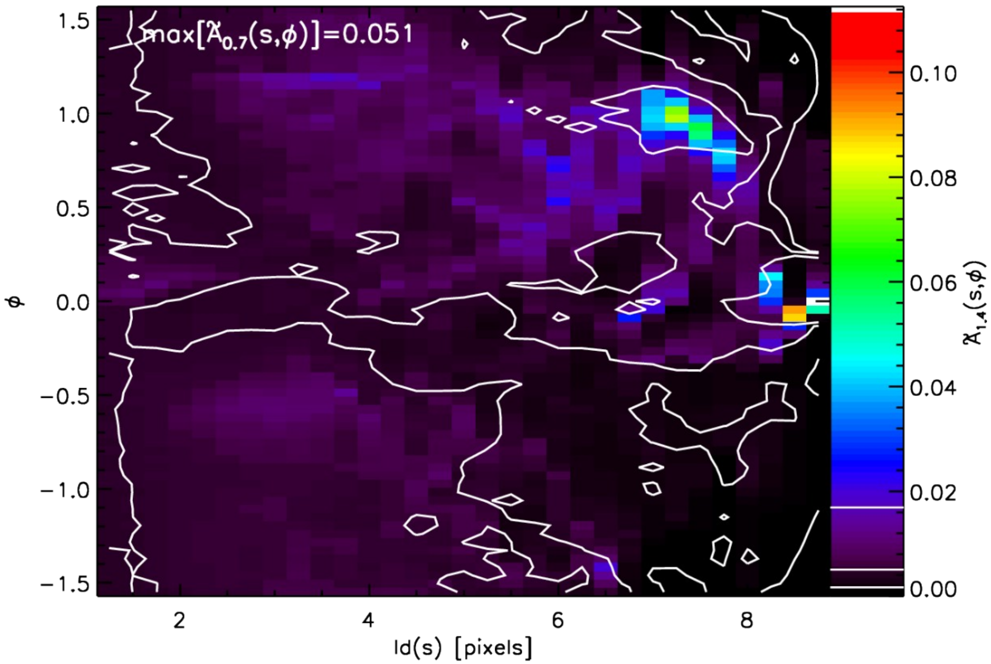

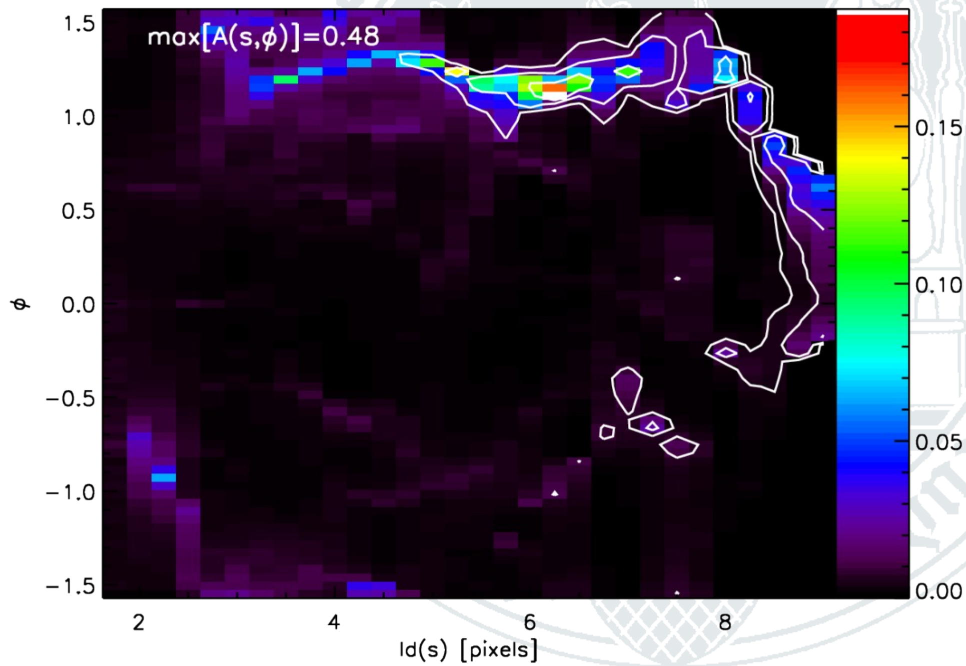

Angular spectra normalized to the isotropic coefficients M^i

- At large scales both maps are dominated by one main filament
- In Aquila the main ridge is the main filamentary structure at all scales
  - Small perpendicular contributions at small scales
- In Polaris filaments at small scales are widely distributed over all angles.

Filament skeleton from the maps of wavelet coefficients

Example: Polaris

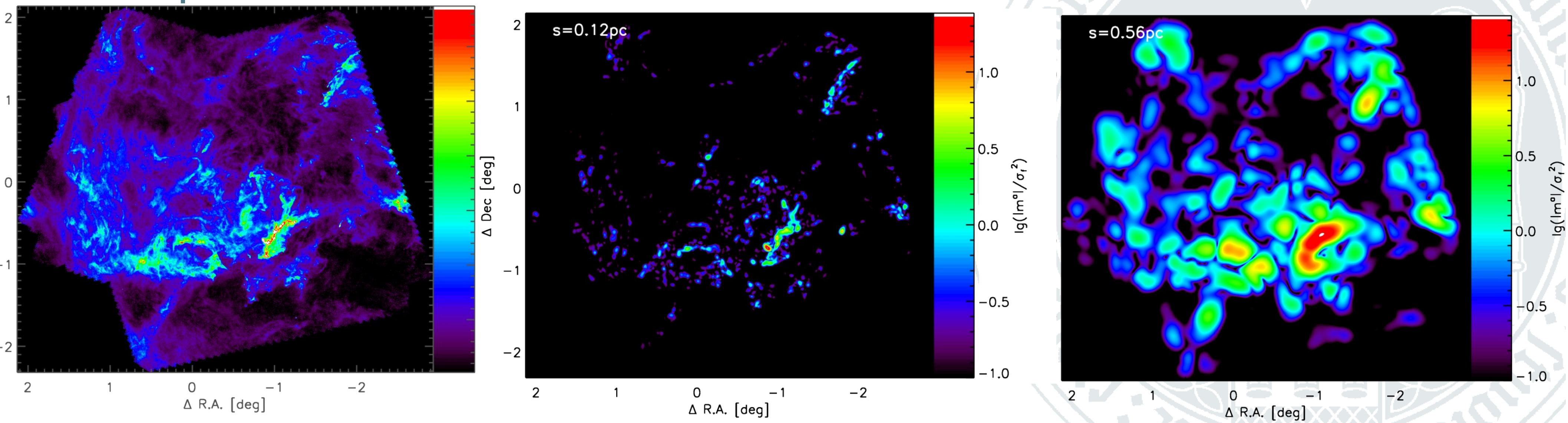

Maps of anisotropic wavelet coefficients for different wavelet sizes. *Left:* 16 pixels = 0.12pc, *Right:* 76 pixels = 0.56pc

- The maps of wavelet coefficients for small filters follow the spines of the filaments identified by eye or one of the traditional filament finders
- The widespread emission and more isotropic structures seen e.g. in the eastern part of the map are filtered out.
- The coefficients for larger filters trace larger and larger filamentary structures that are not necessarily correlated with those at small scales.

Wavelet coefficients measure gravitational stability/instability

- Jeans criterion can be translated into product of column density and core width/filament width

$$\hat{N}R > 3^{1/3}\frac{5}{2\pi}\frac{c_s^2}{G\mu} \approx 1.15\frac{c_s^2}{G\mu} \text{ for spheres}$$

$$\hat{N}R > \frac{4}{\pi}\frac{c_s^2}{G\mu} \approx 1.27\frac{c_s^2}{G\mu} \text{ for cylinders}$$

$$\approx 1.2\times10^{21}\mathrm{cm}^{-2}\mathrm{pc} \text{ at } 15\mathrm{K}$$

- Wavelet coefficients give column density perturbation and size of the perturbation for isotropic and anisotropic modes
- Gravitational stability can be read from the wavelet spectra

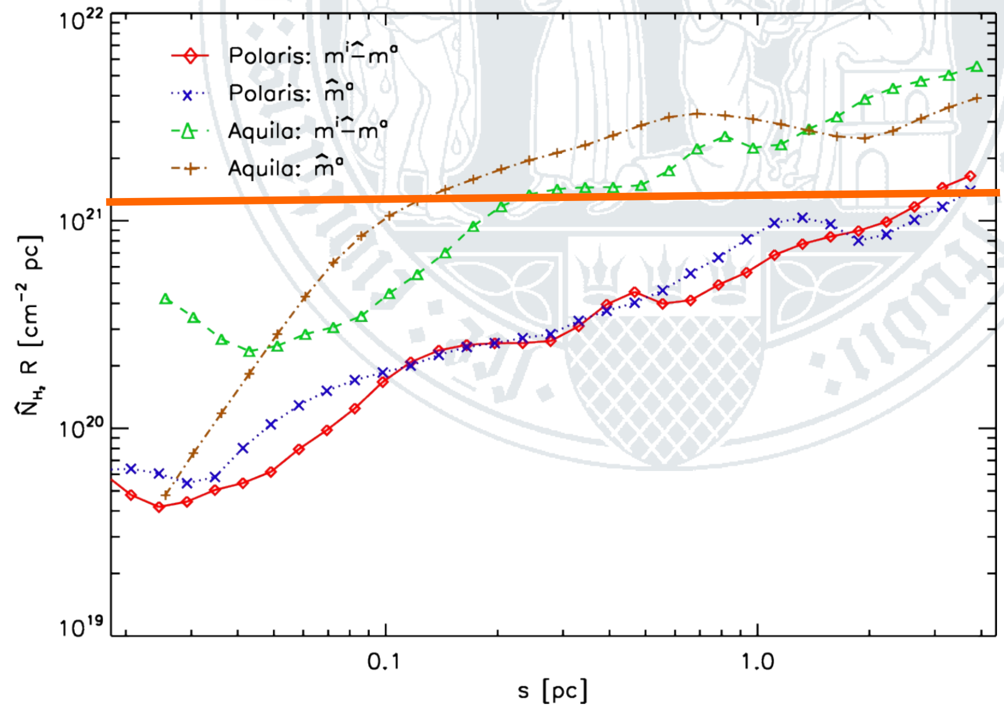

Gravitational mode spectrum for the dominating structures in the observed maps.

- Polaris stable
- Aquila unstable above 0.1pc. Cylindric modes “win” at all scales up to 1.2pc

Gravitational stability

Spatial distribution from map of coefficients

- Scale of supercritical modes give size ($\propto \sqrt{\tau_{\rm ff}}$) of collapsing regions

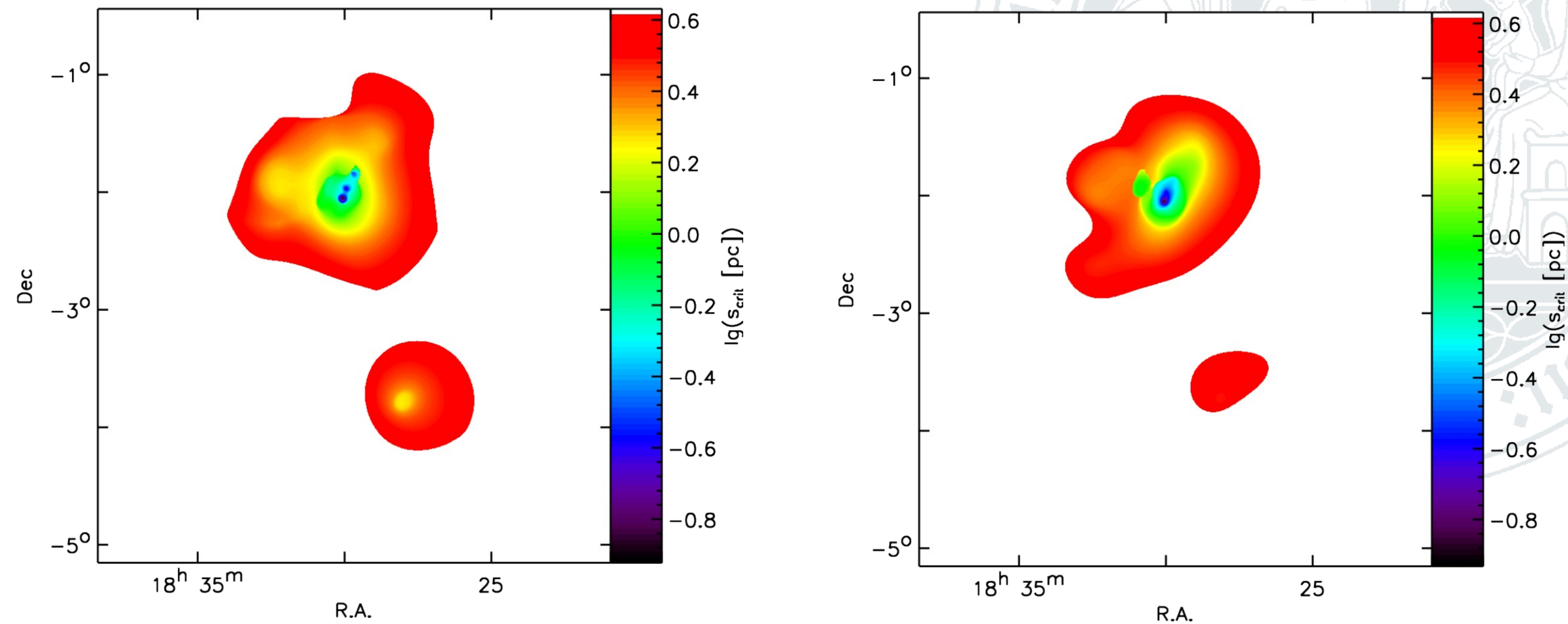

Minimum wavelet scale where stability criterion is exceeded for isotropic modes (left) and anisotropic modes (right) in the Aquila column density map.

- Only the main Aquila filament will undergo quick collapse.
- Cylindrical collapse dominates along the main filament, isotropic collapse at its ends and in the extended environment of the filament.

Summary

Anisotropic wavelets are an unbiased approach to measure filaments

- Provide full spectrum of filament widths from the resolution limit up to about 20 % of the map size.
- Application to MHD simulations
  - Optically thin lines trace small-scale filaments - entangled with the field lines
  - Optically thick lines trace the velocity structure that inherits more of the global anisotropy from the large-scale magnetic field.
- Applications to observed column density maps
  - No characteristic filament width of 0.1pc!
  - Polaris shows filaments of all sizes and directions
  - Aquila has a characteristic FWHM of the main filament of 0.3 pc
  - Spectra give relative importance of spherical and cylindrical collapse modes. In Aquila, the cylindrical modes dominate. Polaris is stable.